Assessment of the Effectiveness of Prestressed NSM CFRP Laminates for the Flexural Strengthening of RC Beams

M. Rezazadeh[1], I. Costa[2], J. Barros[3]

[1]Phd student of department of civil engineering, University of Minho, M.rezazadeh@civil.uminho.pt
[2]Phd student of department of civil engineering, University of Minho, Ines.costa@civil.uminho.pt
[3]Professor of department of civil engineering, University of Minho, Barros@civil.uminho.pt

Keywords: NSM; CFRP; Flexural strengthening; Beams; Prestressing.

SUMMARY

The flexural behavior of RC beams strengthened with prestressed near-surface-mounted (NSM) carbon-fiber-reinforced-polymer (CFRP) laminate was investigated in this paper. For this purpose, four RC beams were tested under monotonic four-point loading. One beam was kept un-strengthened, as a control beam, and another one was strengthened with a non-prestressed NSM CFRP laminate. The remaining beams were strengthened with NSM CFRP laminates prestressed at 20% and 40% of its ultimate tensile strength. The prestressed NSM CFRP laminate technique provided a significant increment of the load carrying capacity for deflection levels corresponding to serviceability and ultimate limit states. A numerical strategy was also employed to simulate the flexural behavior of the tested RC beams. The experimental and numerical researches are described and the relevant results are presented and discussed.

1. INTRODUCTION

Carbon Fiber Reinforced Polymer (CFRP) reinforcements have been showing to be effective to increase the flexural and the shear resistance of reinforced concrete (RC) structures by using the Near Surface Mounted (NSM) strengthening technique [1-3]. NSM is based on introducing CFRP elements into slits opened on the concrete cover of the RC members to strengthen, and bonded to the surrounding concrete with an adhesive [1]. The CFRP laminates of rectangular cross section provide higher strengthening efficacy than round and square cross section bars due to higher ratio between perimeter and cross sectional area, and also due to the higher confinement effectiveness created by the concrete surrounding the reinforcement [4,5]. However, although NSM CFRP laminates can increase the ultimate flexural strength of RC members, they do not significantly increase the load carrying capacity for deflection levels corresponding to the serviceability limit state (SLS). Recent research showed that applying NSM CFRP reinforcements with a certain prestress level can mobilize better the potentialities of these high tensile strength materials, with an appreciable increase of the load carrying capacity of RC beams at SLS [6-9]. However, competitive devices, capable of applying NSM prestressed laminates according to the constraints imposed by real applications still need to be developed. In the present work the preliminary experimental tests with RC beams strengthened according to a technique already proposed [10] are presented. For this purpose, four RC beams were tested under monotonic four-point loading configuration. The influence of the prestressed level on the flexural response of these beams was assessed, with a special focus on the benefits in terms of load carrying capacity at SLS, as well as its influence in the ultimate deflection of the beams. The experimental program is described and the main results are presented and discussed.

Advanced numerical simulations based on the finite element method (FEM) are a competitive alternative to experimental research for the assessment of the effectiveness of the strengthening technique [11,12]. However, for predicting realistically the behavior of RC beams strengthened

according to the new technique, the nonlinear behavior of the material constituents, as well as the CFRP-adhesive-concrete interfaces should be correctly modeled, which is still a challenge in the computational mechanical domain. Furthermore, in the numerical analysis carried out, the realistic prestressing process of the CFRP elements adopted in the experimental tests was simulated. The numerical research conducted is briefly described and the relevant results are presented and discussed.

2. EXPERIMENTAL PROGRAM

The experimental program consisted of four RC beams: a non-strengthened RC beam serving as a control beam, a strengthened RC beam with a non-prestressed CFRP laminate (herein designated as passive CFRP laminate), and two strengthened RC beams reinforced with a NSM CFRP prestressed laminate, one at 20% and the other at 40% of the ultimate tensile strength of the CFRP laminate.

2.1 Geometry, reinforcement, loading and supporting conditions of the beams

The geometry, supporting and loading conditions are schematically represented in Fig. 1a. The RC beams were monotonically tested under four-point loading at a deflection rate of 1.2 mm/min. Each beam was reinforced in the tension and in the compression faces with 2ϕ10 steel bars, and included closed steel stirrups of 6 mm diameter spaced at 80mm to avoid shear failure (Fig. 1b).

For the strengthened RC beams, a groove of 6mm × 24mm cross section was cut on the concrete cover (Fig. 1b) along the total length of the beam. To apply the prestressed CFRP laminate for the strengthening of the RC beams, a CFRP laminate was placed in the groove with no epoxy and then, after applying the prestressing force, the groove was completely filled with the epoxy adhesive. However, in order to simulate the constraints imposed by the supports in real strengthening applications, only 2100mm of the groove was filled with epoxy adhesive, which means that in a length of 150mm in each extremity of the beams the CFRP laminate was not bonded to the concrete. The cross section of the CFRP laminates had 1.4mm of thickness and 20mm of depth.
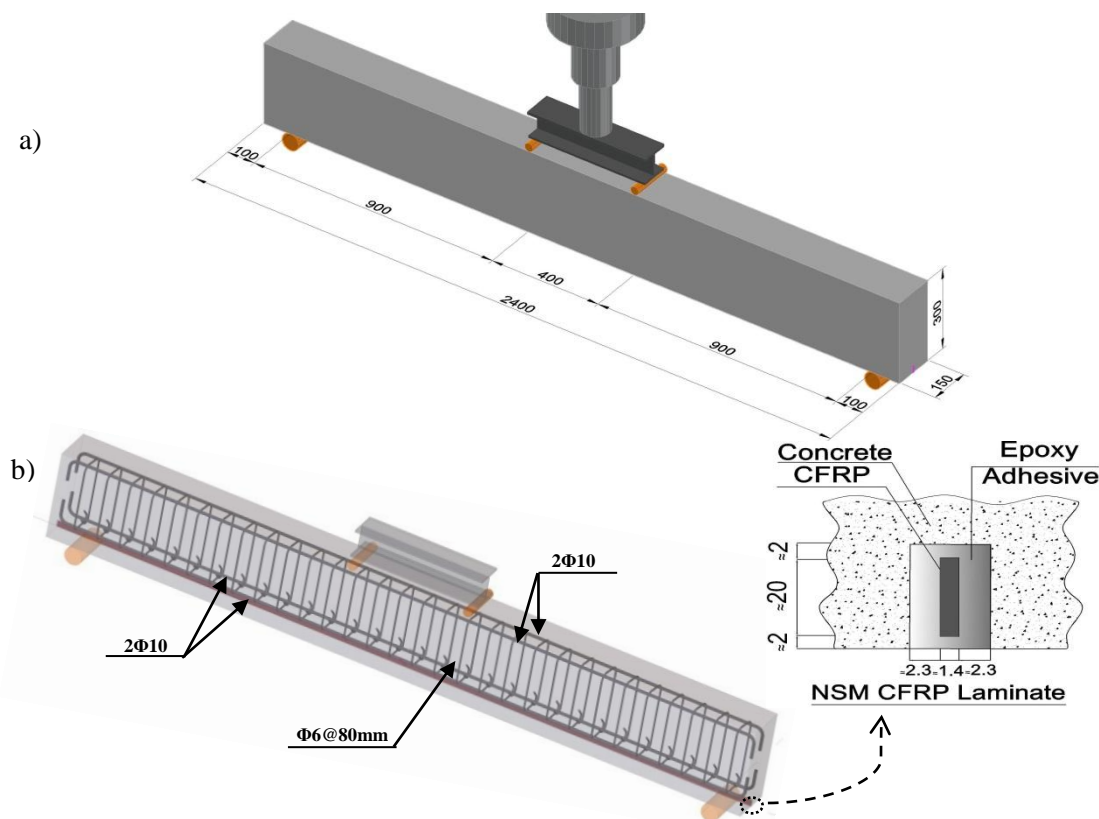

Figure 1: Beams of the experimental program: a) geometry, loading and support conditions, b) reinforcement details

2.2 Material Properties

Table 1 includes the values of the main properties of the concrete, steel bars, CFRP laminate and epoxy adhesive. The average concrete compressive strength and young modulus were evaluated from uniaxial compression tests on cylinders of 150mm diameter and 300mm height [13].

Table 1: Material properties

Material Type	*Number of samples*	*Property*	*MPa*
Concrete	3	Compressive strength at 28 days	21.2 (3.3)
	2	Compressive strength at 153 days[§]	32.2 (1.1)
	3	Young's modulus at 28 days	25.9×10^3 (2.0×10^3)
	2	Young's modulus at the 153 days[§]	27.4×10^3 (2.4×10^3)
Steel Bars	5	Young's modulus of bars ϕ10	208×10^3 (6×10^3)
	4	Young's modulus of bars ϕ6	218×10^3 (8×10^3)
	5	Yield tensile strength of bars ϕ10	516 (3)
	4	Yield tensile strength of bars ϕ6	613 (14)
	5	Ultimate tensile strength of bars ϕ10	636 (4)
	4	Ultimate tensile strength of bars ϕ6	696 (9)
CFRP Laminates	4	Tensile strength	2330 (401)
	4	Elastic modulus	173×10^3 (23×10^3)
Epoxy Adhesive	5	Tensile strength	20.6 (0.7)
	5	Elastic modulus	7.42 (0.29)

Average (Standard Deviation)
[§] 153 days is the age of testing.

2.3 Prestressing

One of the main challenges to use the prestressing system for strengthening of RC beams is the access to the extremities of the beams as support for the actuators which is not feasible in real strengthening applications. In order to overcome this drawback, in 2009 Barros proposed a prestressing system for the NSM-CFRP flexural strengthening of RC elements, which is schematically described in Fig. 2 [10]. The description of this concept can be found in [10], and design details of all the components of this system are available in [14,15].
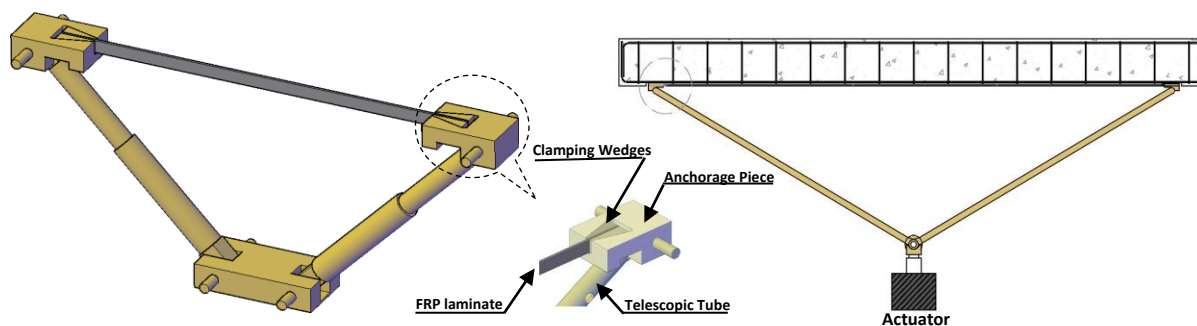

Figure 2: Telescopic device to apply prestressed NSM CFRP laminates

For laboratory conditions, the prestressing system represented in Fig. 3 was designed. The sliding extremity of the prestressing system consists of a hollow hydraulic cylinder with a maximum capacity of 20 ton, to which is connected a through-hole load cell of 200 kN.

For the beams prestressed at a level of 20% and 40% a load of 11.1 kN and 22.8 kN was applied to the laminate, respectively, which corresponds to a stress level of 396 MPa and 814 MPa. During the curing period of the epoxy (72 hours) a maximum fluctuation of 27 MPa was recorded, due to, mainly, temperature variation of the environmental conditions. An average rate of load decay of 0.3 kN/min was imposed for the releasing of the prestress in order to avoid cracking in the surrounding concrete and sliding at the CFRP/adhesive/concrete interfaces.
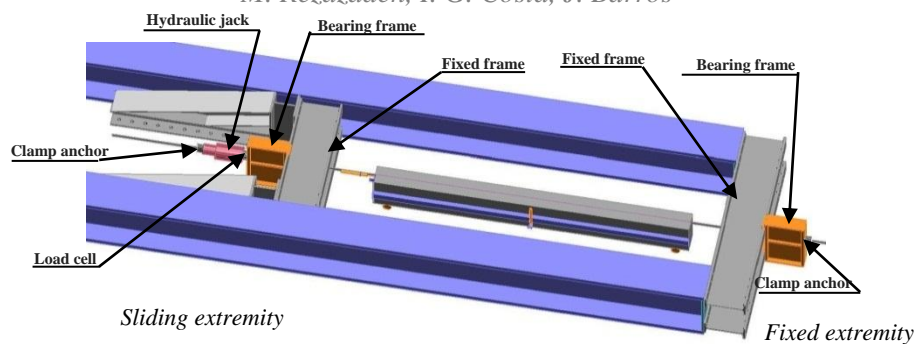
Figure 3: Prestressing system for laboratory experimental programs

3. EXPERIMENTAL RESULTS

3.1. Force-Deflection

The force-deflection relationships for all tested beams are indicated in Fig. 4, where it can be concluded that all the strengthened beams provided an increase of about 60% in terms of the ultimate load carrying capacity, when the control RC beam is considered for comparison purposes. However, at the deflection level corresponding to SLS (8.8mm) [16], the load increment provided by passive, 20% and 40% prestressed CFRP laminates was 32%, 47% and 55%, respectively, revealing the benefits of the prestressing. It is worth noting that the beams prestressed with 20% and 40% exhibited similar behavior in the phase between crack initiation and yielding. This fact can be attributed to the low CFRP reinforcement ratio, as well as to a possible lower concrete tensile strength of the beam reinforced with 40% when compared to the beam prestressed with 20%. However, at the moment of yield initiation, the effect of the 40% prestress is evident since it is visible that the deflection level at which it occurred has increased.
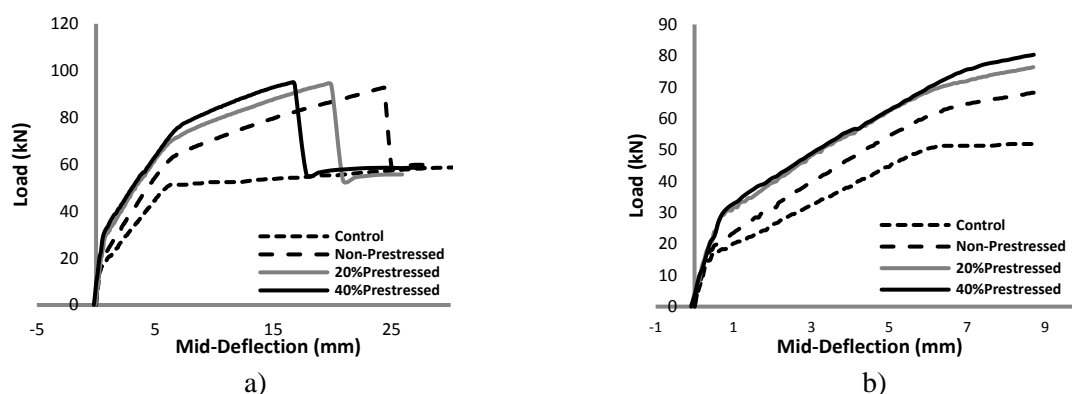

a)

b)

Figure 4: Load-deflection curves of tested beams up to: a) ultimate; b) deflection at SLS

In Table 2, the relevant results obtained in the tests are indicated, where: Δ_i is the initial deflection due to the prestress load; P_{cr} is the load at cracking initiation and Δ_{cr} its corresponding deflection; P_y is the load at yield initiation of the longitudinal tensile bars and Δ_y its corresponding deflection; P_{sr} is the load at SLS; P_u is the ultimate load and Δ_u its corresponding deflection; P_{src} is the load at SLS of control beam.

Table 2: Main results obtained in the tested beams

RC Beams	Δi (mm)	Pcr (kN)	Δcr (mm)	Py (kN)	Δy (mm)	Psr (kN)	Pu (kN)	Δu (mm)	$\dfrac{P_{sr} - P_{src}}{P_{src}}$ (%)
Control	0.00	13.81	0.30	50.42	6.00	51.86	57.12	24.46	0.00
Passive	0.00	16.55	0.35	62.27	6.35	68.32	92.97	24.46	31.74
20%Prestress	-0.08	18.70	0.35	68.16	5.90	76.38	94.00	19.36	47.28
40%Prestress	-0.18	20.73	0.31	74.24	6.61	80.35	95.16	16.92	54.94

3.2 Failure Modes

The crack patterns of all beams consisted predominantly on flexural cracks. However, two distinct types of failure modes were observed: the control beam failed by concrete crushing at top face after yielding of tension steel bars, while all strengthened RC beams failed by rupturing of the CFRP laminate after the yielding of the tension steel bars and before concrete crushing.

3.3 Energy Absorption

To evaluate the energy absorption capability of all the beams, the energy absorption of the tested beams was determined by integrating the area under the force-deflection curves up to the service and ultimate load/deflection (defined in Table 2). The obtained values are indicated in Table 3, where ϕ_{SLS} and ϕ_{ULS} are the energy absorption of the beams up to the service and ultimate load level, respectively, and the subscript c refers to the energy absorption of the control beam. Fig. 5 evidences that the increase in the prestress level enhances the service energy absorption even though the ultimate energy absorption decreases almost linearly with the applied prestress. Nevertheless, for the prestress level of 40%, the energy absorption at ultimate load level is almost equal to the one produced by the control beam. This reveals that, despite the loss energy absorption, the performance of this beam under this prestress level is still significant and it is therefore considered that, for this series of beams, 40% is the optimum prestress level.

Table 3: Energy absorption of beams

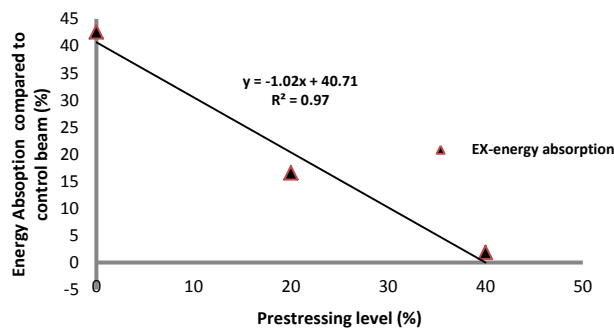| RC Beams	ϕ_{SLS} (kN.mm)	ϕ_{ULS} (kN.mm)	$(\phi_{SLS} - \phi_{SLS,c}) / \phi_{SLS,c}$ (%)	$(\phi_{ULS} - \phi_{ULS,c}) / \phi_{ULS,c}$ (%)
Control	335.2	1183.0	0.0	0.0
Non-Prestress	414.8	1687.0	23.7	42.6
20% Prestress	473.7	1379.0	41.3	16.6
40% Prestress	488.4	1205.1	45.7	1.9

Figure 5: Ultimate energy absorption of beams compared to control beam

4. NUMERICAL MODELING

4.1 FE Model Description

A 3D finite element model was used to simulate the behavior of the tested beams. 3D eight-node solid elements were used to model the concrete, CFRP laminate and epoxy adhesive. 3D two-node truss elements were adopted to model the steel bars. To reduce the computational time, a quarter of the full size beam was modeled, taking the advantage of the double symmetry of the beams. The loading and boundary conditions of the model were applied according to the particularities of the test setup. Preliminary analyses were carried out in order to obtain a mesh refinement that does not compromise the accuracy of the simulations. Furthermore, a fine mesh refinement was applied in the zones where relatively high stress gradients are expected to occur, and the final mesh is depicted in Fig. 6.
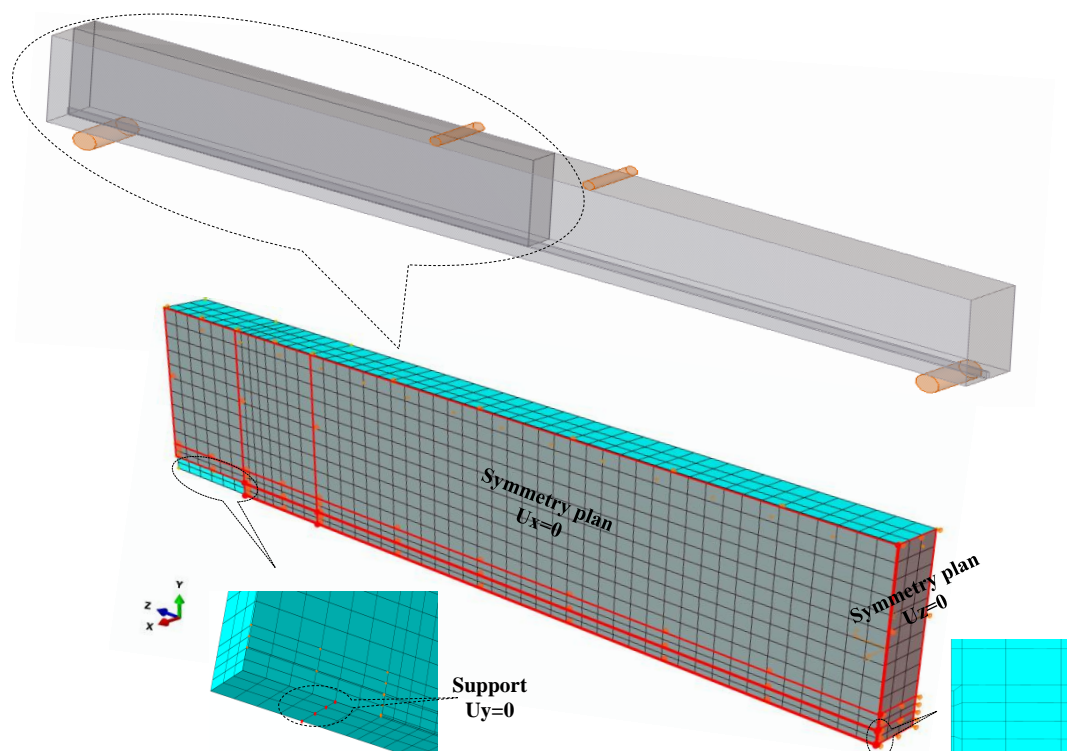
Figure 6: Finite element mesh of the tested beams (a quarter of the beam was selected)

The Nonlinear Concrete Damaged Plasticity (CDP) model was selected to simulate the concrete nonlinear behavior [22]. In this CDP model, the concepts of linear isotropic elasticity in combination with isotropic tensile and compressive plasticity are used to simulate the inelastic behavior of the concrete. The CDP model considers non-associated potential plastic flow resulting in a non-symmetric stiffness matrix. The Drucker-Prager hyperbolic function was used to assess the flow potential [22]. The CDP model assumes that tensile cracking and compressive crushing of the material are the two main failure mechanisms. The concrete stress-strain relation for uniaxial compression was obtained according to the recommendations of CEB-FIP model code [17]. To describe the concrete tensile behavior, a linear stress-strain relation was assumed for uncracked concrete, and a stress-crack opening relation according to CEB-FIP model code was used for the cracked concrete (with tensile fracture energy, G_{ftc}, of 0.08 N/mm) [17].

The values of the CDP model parameters were estimated based on the recommended range of values, by determining those that assure the best prediction of the force-deflection recorded in the experimental test with the control beam [18-22]. These parameters, used in the numerical simulations, were determined as follows:

- Dilation angle, ψ: is the inclination of the failure surface towards the hydrostatic axis, measured in the meridional plane. It is physically explained as the concrete internal friction angle and it usually ranges between 36º and 40º [21]. In the numerical simulations, the value of 38º was adopted;

- Plastic potential eccentricity, e: adjusts the shape of meridional plane (herein assumed as a hyperbola) at which the function approaches an asymptote, meaning that the flow potential tends to a straight line in the meridional plane as the eccentricity tends to zero [21-22]. This eccentricity can be considered equal to the ratio between tensile and compressive strength of concrete or, in alternative, 0.1 as recommended by CDP model [21];

- Stress ratio f_{b0}/f_{C0}: is the ratio between the initial biaxial compressive yield stress and the initial uniaxial compressive yield stress, which was taken as 1.16, as recommended by CDP model [22]

- Shape of the loading surface, K_c: describes the ratio of the distance between the hydrostatic axis and the compression meridian and the tension meridian in the deviatoric cross section, respectively [21]. K_c ranges between 0.5 and 1 and the CDP default value of 2/3 was assumed in the analyses;

- Viscosity parameter, VP: it was assumed to be zero in the analyses.

Elasto-plastic models with associated plastic flow were used to simulate the behavior of epoxy adhesive and steel bars. This means that the inelastic deformation rate is normal to the yield surface [22]. The perfect plasticity model, with no hardening, was used to simulate the epoxy adhesive behavior. On the other hand, the isotropic hardening plasticity model was considered to simulate the behavior of steel bars up to its ultimate tensile strength in agreement with the results of the tensile tests. A linear elastic stress-strain relation up to the ultimate tensile strength was adopted to simulate the tensile behavior of the CFRP laminates.

To simulate the bond behavior of the CFRP laminate-adhesive-concrete interfaces, two surface-based contact interfaces were defined. One was used at the laminate-epoxy adhesive interface, while the other was applied at the concrete-epoxy adhesive interface. A mixed mode of debonding including stress-separation (in the normal direction of the interface element) and shear stress-slip (on both directions of the interface element plane) was used to simulate the concrete-epoxy adhesive interface, while for the laminate-epoxy interface only the shear stress-slip, in both directions of the plane, was considered. A linear softening law was defined to describe damage evaluation in the interface.

To describe the shear stress-slip behavior in the interface between the epoxy adhesive and the concrete, the values of the maximum shear stress (τ_{max}), maximum shear slip (δ_{max}), and the shear fracture energy (G_{fs}) were obtained from Eqs.(1-3) [23].

$$\tau_{max} = (0.802+0.078 \cdot \varphi) \cdot f_c^{0.6} \tag{1}$$
$$\delta_{max}=(0.976 \cdot \varphi^{0.526}) / (0.802+0.078 \cdot \varphi) \tag{2}$$
$$G_{fs}= (\tau_{max} \cdot \delta_{max})/2 \tag{3}$$

where φ is the aspect ratio of the interface failure plane defined as (groove depth+1mm)/(groove width+2mm), and f_c is the concrete compressive strength. According to these equations and the geometric/material characteristics of the beams previously described in section 2, the values of τ_{max}=8.4 MPa, δ_{max}=1.7 mm, and G_{fs}=7.1 N/mm were used for the shear stress-slip model.

Concerning the stress separation components, the maximum tensile stress of the interface was limited to the concrete tensile strength and, therefore, failure is assumed to occur in the surrounding concrete when the tensile stress exceeds the concrete tensile strength (σ_{tc}) [12]. The tensile fracture energy was considered to be equal to the fracture energy of concrete (G_{ftc}). So, the values of σ_{tc}=2.51 MPa and G_{ftc}=0.08 N/mm were used for modeling the normal stress-separation behavior.

To model the interface between the epoxy adhesive and the CFRP laminate, the following shear stress-slip law was used [24]:

$$\tau(s) = \begin{cases} \tau_m \left(\dfrac{s}{s_m} \right)^{\alpha} & s \leq s_m \\[4mm] \tau_m \left(\dfrac{s}{s_m} \right)^{-\alpha'} & s > s_m \end{cases} \tag{4}$$

where τ_m and s_m are the maximum shear stress and its corresponding slip, respectively, and α and α' are parameters defining the shape of the pre- and post-peak τ-s curves. The values of these parameters were found in literature [24] for concrete with similar strength. The shear fracture energy of this interface was estimated to be equal to the area under the shear stress-slip curve, imposing 1.7 mm as the maximum admissible slip. Thus, the values of α=0.16, α'=0.32, s_m=0.23 mm, τ_m=20 MPa and G_{fs}=23.56 N/mm were used for defining the shear bond-slip model.

These equations were selected due to their simplicity and ability to simulate appropriately the bond behavior between epoxy adhesive and both CFRP laminate and concrete.

The following four steps of the experimental tests were simulated numerically in order to reproduce, as much as possible, the real test conditions:

Step 1: Applying prestressing force on the CFRP laminate.

Step 2: Introducing the interfaces between concrete/epoxy adhesive and CFRP laminate/epoxy adhesive, assuming that the properties of the interfaces correspond to a hardened stage of the epoxy.

Step 3:   Release the prestressing force.
Step 4:   Applying the monotonic load up to the collapse of the beam.

4.2 Assessment of the predictive performance of the numerical strategy
Fig. 7 compares the force versus mid span deflection obtained numerically and experimentally. The obtained results show the high predictive performance of the adopted numerical strategy.
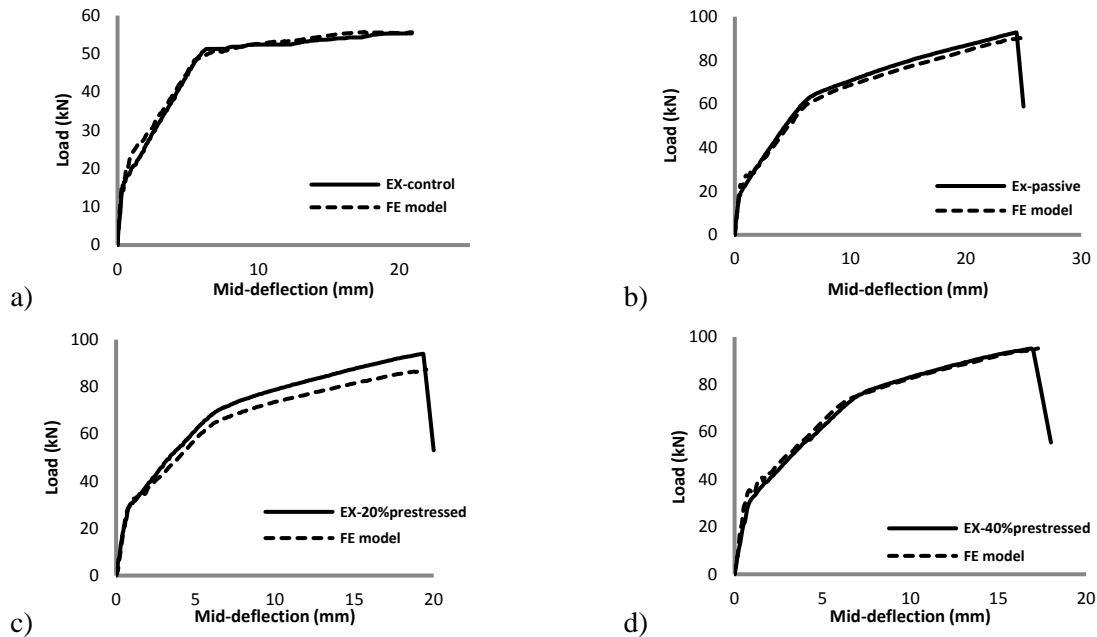

Figure 7: Comparison between experimental and numerical load-mid deflection curves,
a) Control beam, b) Non-prestressed beam, c) 20% prestressed beam, d) 40% prestressed beam

The good predictive performance is also evidenced in Fig. 8, where the relationship between the applied load and the tensile strain in the laminate, measured at mid-section of the beam, is represented.
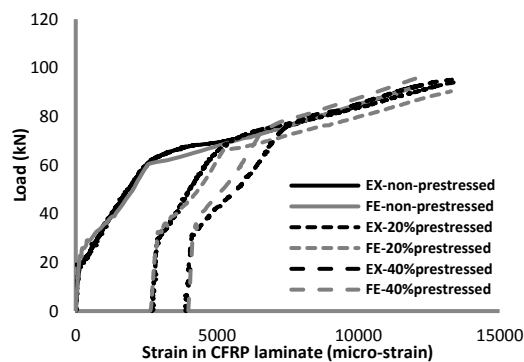

Figure 8: Load versus strain in CFRP laminate at mid-section of the beam

The comparison between the experimental and the numerical ultimate energy absorption curves with respect to the control beam is presented in Fig. 9. The best prestress level obtained from FE analysis was 36.6%, which is in good agreement with the experimental one ($\cong$40%).
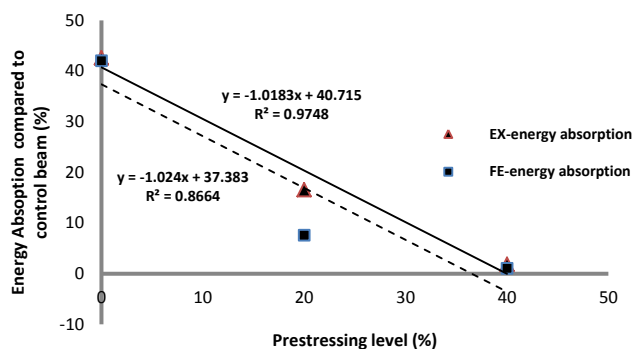
Figure 9: Comparison between experimental and numerical energy absorption capacity of the strengthened beams

5. CONCLUSIONS

A strengthening technique based on applying prestressed CFRP laminates into slits cut on the concrete cover was used with the purpose of increasing the load carrying capacity of RC beams failing in bending, mainly at serviceability limit state conditions. A nonlinear 3D finite element model was used to predict the flexural behavior of the tested beams. According to this research, it can be concluded that:

1. A CFRP reinforcement ratio of $\rho_f = A_f / (b\, d_f) = 0.06\%$ has conducted to an increase of about 63% in the ultimate load carrying capacity of beams with a steel reinforcement ratio of $\rho_s = A_s / (b\, d_s) = 0.39\%$, regardless the fact the CFRP laminate is passive or applied with a prestress level of 20% and 40%.

2. A prestress level of 20% and 40% conducted to an increase of 47% and 55% in terms of load carrying capacity at deflection corresponding to the serviceability limit state, while passive CFRP laminate provided an increase of 32%.

3. Prestressing of NSM CFRP laminate was effective in terms of increasing the load at crack and steel yield initiation.

4. When compared to the energy absorption of the control beam, the strengthened beams exhibited a linear decreasing of the energy absorption with the increase of the prestress level.

5. Considering the criteria of preserving the energy absorption capacity of the control beam with the highest increase of load carrying capacity for serviceability limit state conditions, a prestress level of 40% seems to be the most appropriate for the tested series of beams.

6. Since all the strengthened beams failed by the rupture of the CFRP laminate, the used epoxy adhesive provided proper bond conditions between adhesive and both the surrounding materials: CFRP laminate and concrete.

7. The proposed 3D finite element approach that simulates concrete/ adhesive and laminate/ adhesive interfaces simultaneously, as well as the relevant nonlinear features of the intervening materials, has predicted with high accuracy the deformational response of the tested beams, as well as relevant results determined experimentally.

REFERENCES

[1] J.A.O. Barros and A.S. Fortes, "Flexural strengthening of concrete beams with CFRP laminates bonded into slits", Journal Cement and Concrete Composites, 27(4) p. 471-480, (2005).

[2] J.A.O. Barros and S.J.E. Dias and J.L.T Lima, "Efficacy of CFRP-based techniques for the flexural and shear strengthening of concrete beams", Journal Cement and Concrete Composites, 29(3), 203-217 (2007).

[3] S.J.E. Dias and J.A.O. Barros, "Experimental behaviour of RC beams shear strengthened with NSM CFRP laminates", Strain - An International Journal for Experimental Mechanics, 48(1), 88-100, February 2012.

[4] R. El-Hacha and S.H. Riskalla, "Near-surface-mounted fiber-reinforced polymer reinforcements for flexural strengthening of concrete structures", ACI Structural Journal, 101(5), 717-726 (2004).

[5] A. Palmieri and S. Matthys and J.A.O. Barros and I.G. Costa and A. Bilotta and E. Nigro and F. Ceroni and Z. Szambo and G. Balazs, "Bond of NSM FRP strengthened concrete: Round Robin Test Initiative", CICE 2012 6th International Conference on FRP Composites in Civil Engineering, 8pp., Rome, Italy, 13-15 June 2012.

[6] H. Nordin and B. Taljsten, "Concrete Beams Strengthened with Prestressed Near Surface Mounted CFRP", Journal of Composites for Construction, 10(1), January/February, pp. 60-68 (2006).

[7] M. Badawi and K. A. Soudki, "Fatigue of RC beams strengthened with prestressed NSM CFRP rods", Fourth International Conference on FRP Composites in Civil Engineering (CICE2008), Zurich, Switzerland, 22-24 (2008).

[8] M. Badawi and K. Soudki, "Flexural Strengthening of RC Beams with Prestressed NSM CFRP Rods- Experimental and analytical Investigation", Journal of Construction and Building Materials, 3292-3300, (2009).

[9] F. Oudah and R. El-Hacha, "Ductility of Reinforced Concrete Beams Strengthened using Prestressed NSM CFRP Strips/Rebars- Analytical Study", First Middle East Conference on Smart Monitoring, Dubai, UAE, (2011).

[10] J.A.O. Barros, "Pre-stress technique for the flexural strengthening with NSM-CFRP strips", 9th International Symposium on Fiber Reinforced Polymer Reinforcement for Concrete Structures, Sydney, Australia, artigo 85, 13-15 July, 2009.

[11] R. A. Hawileh, "Nonlinear Finite Element Modeling of RF Beams Strengthened with NSM FRP Rods", Journal of Construction and Building Materials, (2011).

[12] H. Y. Omran and R. El-Hacha,"Nonlinear 3D FE Modeling of RC beams Strengthened with Prestressed NSM-CFRP strips", Journal of Construction and Building Materials, 74-85, (2011).

[13] E365 (1993). "Hardened Concrete - Determination of the modulus of elasticity of concrete in compression." National Laboratory for Civil Engineering Specification, 2 pp (in portuguese).

[14] I.G. Costa and J.A.O. Barros, "Design and development of hydraulic-electro-mechanical system to apply pre-stressed CFRP laminates according to the NSM technique in laboratory conditions", Technical Report nº 12-DEC/E-10, University of Minho, 59 pp, March 2012.

[15] M. Rezazadeh and J.A.O. Barros and I.G. Costa, "Design details of a pre-stressing system for the NSM strengthening technique of RC elements", Technical Report no 12.DEC/E, University of Minho, 2012.

[16] EN 1992-1-1. Design of concrete structures. Part 1-1: General rules and rules for buildings, 2004.

[17] CEB-FIP model code 2010. Final draft 2011.

[18] T. Jankowiak and T. Lodigowski, "Identification of Parameters of Concrete Damage Plasticity Constitutive Model", Foundation of civil and environmental engineering, No. 6, (2005).

[19] R. Malm, "Predicting Shear Type Crack Initiation and Growth in Concrete with Non-linear Finite Element Method", Royal Institute of Technology (KTH), Stockholm, Sweden, 2009.

[20] W. Lorence and R. Ignatowicz and E. Kubica, "Numerical Model of Shear Connection by Concrete Dowels", Structural Engineering, Mechanics and Computation 3.

[21] P. Kmiecik and M. Kaminski, "Modeling of Reinforced Concrete Structures and Composite Structures with Concrete Strength Degradation Taken into Consideration", Archives of civil and mechanical engineering, Wroclaw University of Technology, No.3, Poland, 2011.

[22] ABAQUS: Abaqus analysis user's manual, Version 6.11, 2011, Dassault Systemes.

[23] R. Seracino and M. R. R. Saifulnaz and D. J. Oehlers, " Generic Debonding Resistance of EB and NSM Plate-to-Concrete Joints", Journal of Composites for construction (ASCE), Vol.11, No.1, 2007.

[24] J. S. Cruz and J. Barros, "Modeling of Bond between Near Surface Mounted CFRP Laminate Strips and Concrete", Journal of Computers and Structures, 1513-1521, (2004)